J Mater Sci (2007) 42:834–840
DOI 10.1007/s10853-006-0075-y

Hot compression and fracture toughness of HSS composed hot strip work rolls

Abdelylah Benazza · Abdelkader Ziadi · Boualem Serier · Belabbes Bachir Bouiadjra · Benali Boutabout

Received: 21 September 2005 / Accepted: 27 March 2006 / Published online: 3 January 2007
© Springer Science+Business Media, LLC 2007

Abstract The rolls in the finishing stands must have good resistance to both wear and fire cracks. The use of high-speed steel at the finishing stands has shown satisfactory results. The composition of this high-alloyed steel is an important parameter as the most significant change lays on the type, morphology, and volume fraction of the eutectics carbides. The heat treatment of these products consists of high temperature austenization followed by quenching and two temperings, as required in order to increase their overall hardness and to completely eliminate residual austenite. The influence of tempering temperatures on the mechanical properties of these products, determined using tensile, hot compression and fracture toughness tests, was studied in this research work. Their corresponding failure micromechanisms were defined by means of the analysis of fracture surfaces.

Introduction

Rolling mill productivity, as well as the surface quality, shape and roughness of the rolled product, are all directly affected by the period of time the roll can be in operation without being removed due to deterioration. Such roll deterioration may be due to wear, oxidation, extensive cracks or even roll fracture. The rolls in the finishing stands must have good resistance to both wear and fire cracks. A compound roll with the outer layer made of high alloyed steel corresponding to the family of alloys used for cutting tools, which is called High Speed Steels (HSS) rolls was developed and HSS rolls were introduced into hot strip mills in Japan in the early 1990s. This new roll has spread all over the mills in Japan quite quickly, even over many mills such in Europe and USA, to replace the Hi-Cr rolls used in the first Finishing stands [1].

High-speed steels are important tool materials due to the fact that they offer a wide spectrum of tailoring properties [2]. These steels have been developed to improve the quality and productivity of rolled goods in accordance with industrial demands. They are characterized by excellent hardness by their good wear resistance, excellent surface roughening resistance and high temperature properties, to be used under more severe conditions than the rolled steel used at present [3]. High speed steel are obtained from a microstructure characterized by a high content of primary and eutectic carbides dispersed in a tempered martensitic phase [4, 5]. The currently increasing request demand for greater productivity and product quality has led to the development of higher performance materials. High-speed steels are manufactured by adding important percentages of carbide-forming elements, such as chromium, vanadium, molybdenum, tungsten, etc., in order to obtain a microstructure composed of carbides with an extreme hardness dispersed in a matrix that still contains a sufficient percentage of carbon to allow a large increase in hardness as a consequence of the complete transformation of austenite into martensite that occurs in a quenching and tempering heat treatment [6]. The

A. Benazza · A. Ziadi (✉) · B. Serier · B. B. Bouiadjra · B. Boutabout
Department of Mechanical Engineering, University of Sidi Bel Abbes, Sidi Bel Abbes 22000, Algeria
e-mail: aekziadi@yahoo.com

shaping of all these products is carried out by means of casting technologies, directly after the elaboration of the alloy in a liquid state. The solidification of high-speed steels starts with the nucleation of austenite dendrites and then continues with the formation of different eutectic constituents (γ + MC, in high niobium and vanadium castings, γ + M7C3, when they have a high chromium content, γ + M2C and γ + M6C, in the case of high tungsten and molybdenum castings). During cooling, significant quantities of these same carbides precipitate as a result of the typical loss in solubility of the austenite as the temperature is reduced [7].

As to HSS rolls used on plate finish rolling mills, fracture toughness and wear resistance are very important properties. During rolling process of the rolls, microcracks often initiate in and proceed along hard carbides distributed in microstructures. Fracture toughness is generally used for evaluating structural stability of materials and is considered to be one of the most important material properties. Correlation studies of fracture toughness and microstructural characteristics, particularly the microfracture mechanism based on the microstructural control of each material concerned, are required to improve fracture toughness [8]. HSS rolls can be fractured unexpectedly by spalling or thermal fatigue caused by the growth of internal cracks or by the roughening of the roll surface. This results from the repeated formation of thermal-fatigue cracks and from the repeated impact load and the increased rolling load caused by abrupt intrusion of rolled plates [9–12]. Though wear resistance of work rolls can be improved by promoting a large amount of hard carbides and plate-type tempered martensite in the matrix, fracture toughness can be deteriorated because of their brittleness. Therefore, to be applicable to more various roll stands, it is essential to improve the overall properties such as hardness and fracture toughness by adjusting shape, volume fraction, distribution of carbides through controlling the casting process, and to enhance the matrix characteristics through controlling heat treatment [13].

The heat treatment of these products consists in austenitization at a high enough temperature so as to dissolve most of the carbides that had precipitated in the previous cooling. A high-alloyed austenite with high carbon content is obtained that is partially transformed into martensite by an appropriate quench. However, an important fraction of retained austenite remains after the hardening treatment that must be completely eliminated by applying two or more tempering heat treatments. In the course of these tempering treatments, a significant structural hardening takes place (secondary hardening) that is related to a uniform precipitation of very fine carbides, along with the transformation of retained austenite into martensite. Finally, after two or even three tempering treatments, a final hardness of between 600 HV and 800 HV can be obtained [14, 15].

Experimental procedure

The chemical composition of the high speed steel used in this work is shown in Table 1.

This high-alloyed steel was austenitized, quenched and finally double tempered. In our experimental study, different tempering temperatures were used with the aim of modifying the final hardness of the product within a practical range. Figure 1 shows the typical microstructure of these high alloyed steels, characterized by a dendritic tempered martensite phase in a matrix of MC, M_7C_3 and M_6C eutectic carbides.

Figure 2 shows the variation in high speed steel hardness with the tempering parameter, $P = T(20 + \log t)$, determined throughout our experiments and which takes into account the combined effect of temperature (K) and time (h) of the two tempering treatments. The figure shows the continuous decrease in hardness with the tempering parameter.

Any significant microstructure differences can be appreciated among these four treatments. The main effect of increasing tempering temperature (Tl to T4) is the growth of the small carbides that precipitate in the course of this heat treatment.

Tensile, hot compression and fracture toughness tests were carried out on each of these four products. Tensile tests were performed according to ASTM E8M-92 [16] standard on cylindrical specimens with a diameter of 6 mm and a calibrated length of 60 mm, under a strain rate of 1 mm/min.

Hot compression tests were carried out at 500 °C, according to ASTM E9 [17] and E209 standards, on specimens with a diameter and length of 5 mm and a 6 mm, respectively, under a strain rate of 1 mm/min. Specimens extracted in the radial and transverse directions of the product were used. These tests were

Table 1 Chemical composition of the product (in weight)

% C	% Mn	% Si	% S	% P
1.5–1.9	0.5–0.7	0.9–1.1	<0.025	<0.025
% Ni	% Cr	% Mo	% W	% V
0.7–0.9	5.0–7.0	3–4	1.5–2.5	4–5

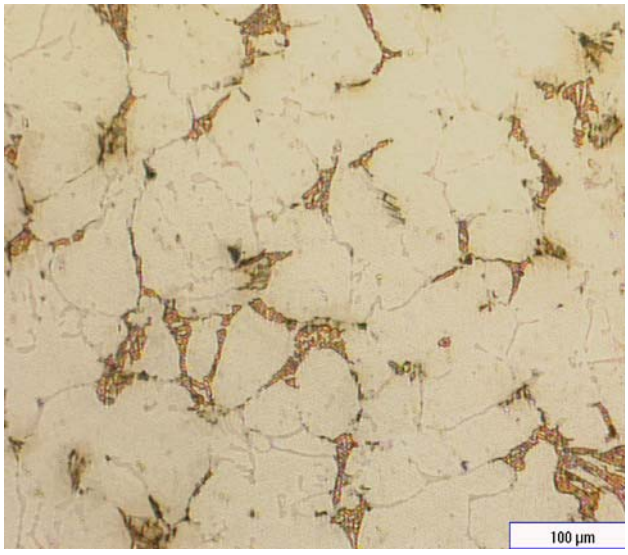

Fig. 1 Microstructure of the heat-treated multi-component cast iron

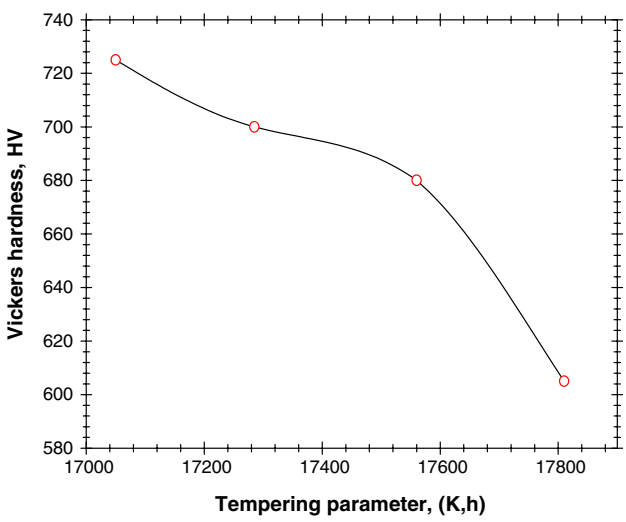

Fig. 2 Evolution of Vickers hardness with the tempering parameter

carried out with the assistance of a furnace equipped with a temperature controller, which was incorporated to the testing machine so as to heat the specimens at a heating rate of 5 °C/min until attaining 500 °C. This temperature was then maintained during 30 min before commencing the compression test. Subsequently, a specimen-less test was carried out under the same conditions to determine the deformation behavior of the unit blocks and bars used to apply of the load and, by subtraction, to obtain the real deformations of the specimens.

Finally, the tests for the determination of the fracture toughness were carried out according to ESIS P2-92 [18] and ASTM E399-90 [19] standards on SENB specimens with a cross-section of 15 mm× 15 mm. All the specimens were precracked by fatigue, in accordance with the standards. Stress intensity factor K_I due to external load P was determined using the following equation:

$$K_I = K_Q = \frac{P_Q \cdot S}{B \cdot \sqrt{W^3}} \cdot f(a/w) \quad (1)$$

where

$$f(a/w) = \frac{3(a/w)^{0.5} \cdot (1.99-(a/w)(1-(a/w)) \cdot (2.15-3.93(a/w)+2.7(a/w)^2))}{2 \cdot (1+2(a/w))(1-(a/w))^{3/2}}$$

Results and discussion

Tensile tests

Table 2 shows the results of the tensile tests (tensile strength, σ_R, failure elongation, A and reduction of area, Z) along with the Vickers hardness obtained in all these heat treatments. It is worth noting the extremely low ductility of all these products and the significant strength reduction of the high speed steel tempered at the highest temperature (T4), which also presented the lowest hardness values.

Examination of the failure surfaces of these specimens by SEM always showed an intergranular fracture associated to the carbide network, which constituted the matrix phase of these high speed steels (Figs. 3, 4). However, any significant difference was observed among the various heat treatments carried out.

Hot compression tests

The results of the compression tests are shown in Fig. 5 and Table 3 (yield strength, σ_y, compressive strength, σ_R, and deformation at failure, A).

As no important difference was observed between the radial and tangential specimens, the results that are presented in Table 3 refer to the specimens extracted in the radial direction. On the other hand, as mentioned in the experimental procedure, the graphs in Fig. 5 and all the values of deformation at failure, A,

Table 2 Results of the tensile tests

Heat treatment	HV	σ_y (MPa)	A (%)	Z (%)
T1	725	748	0.30	0.23
T2	700	782	0.37	0.27
T3	680	—	—	—
T4	605	647	1.00	0.50

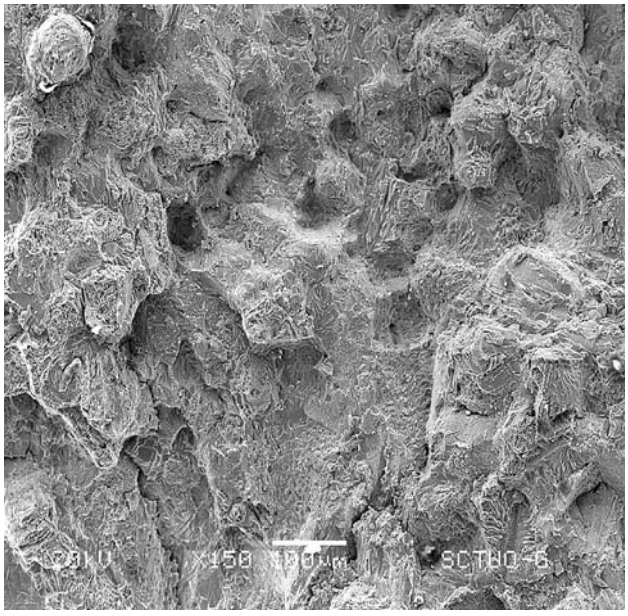

Fig. 3 General pattern of fractured surfaces in the tensile tests (T2)

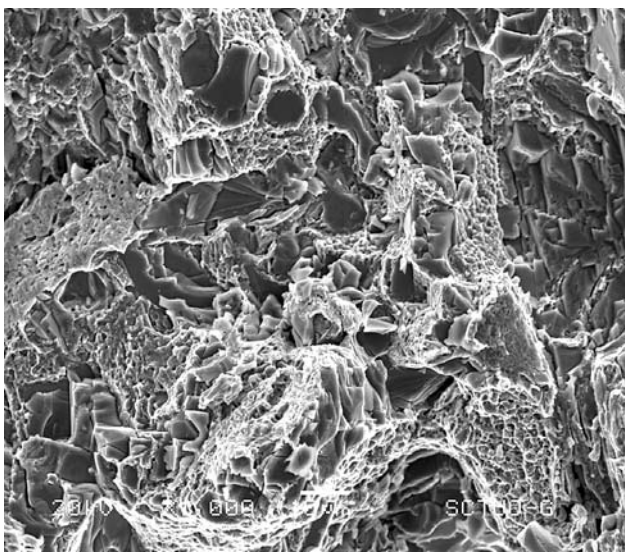

Fig. 4 Detail of the tensile test fractured surface (T3)

were corrected by means of a specimen-less test carried out under the same conditions as the others.

The excellent behaviour that these high speed steels displayed in the compression tests carried out at 500 °C is worth noting. This was characterized by very high values of yield and compressive strength, along with a relatively ductile behaviour, as most of these specimens showed plastic deformations at failure higher than 10. Figure 6, on the other hand, highlights the existing proportionality between the compressive strength at

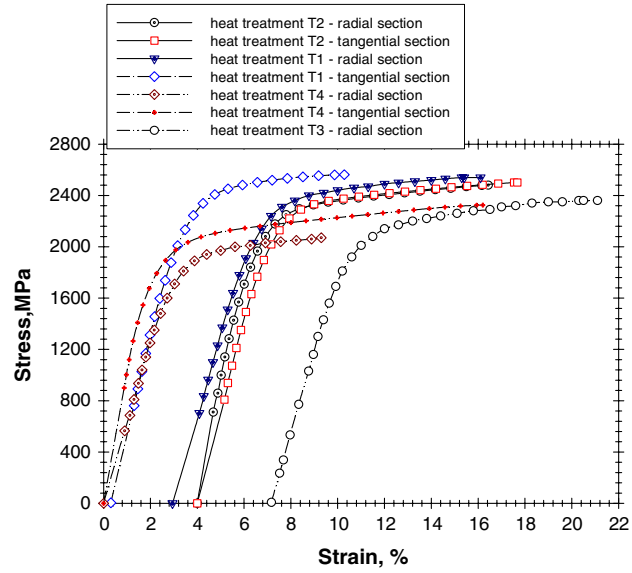

Fig. 5 500 °C compression stress–strain curves once the flexibility of the testing machine and accessories has been corrected

Table 3 Results of compression tests at 500 °C

Heat treatment	HV	σ_y (MPa)	σ_R (MPa)	A (%)
T1	725	1,982	2,546	12.5
T2	700	1,800	2,481	13
T3	680	1,777	2,362	9.5
T4	605	1,640	2,069	14

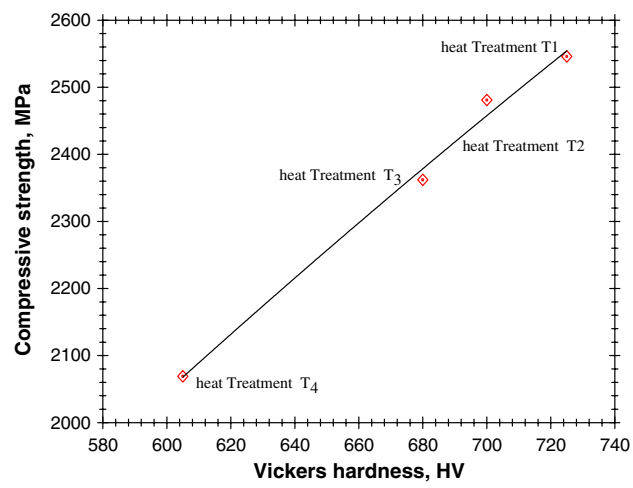

Fig. 6 Relation between Vickers hardness at room temperature and compressive strength at 500 °C

500 °C and the product hardness measured at room temperature.

Failure of hot compression specimens always took place through a smooth plane located at 45° of the axis of load application, the maximum shear stress plane.

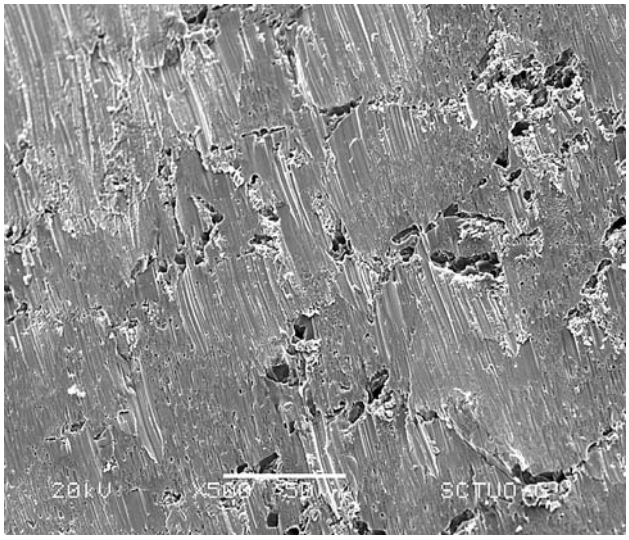

Fig. 7 Typical failure surfaces in 500 °C compression tests

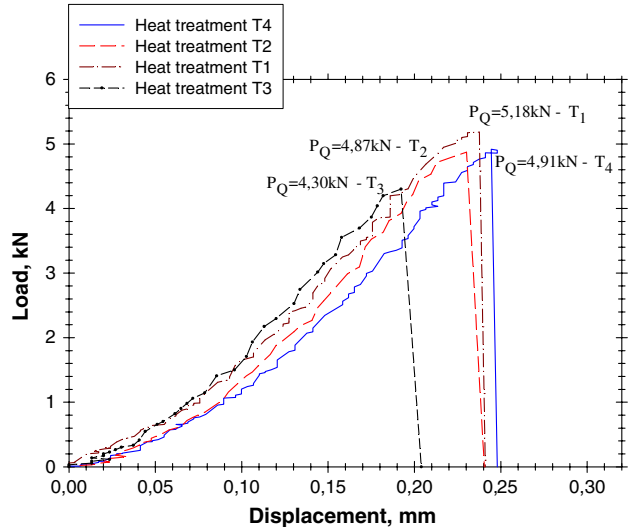

Fig. 8 Load–displacement curves to determine fracture toughness

The failure surface, which is presented in Fig. 7, is very flat and shows hardly any characteristic morphological detail, except for large cavities promoted by the growth after debonding of the interphases between carbides and the dendritic globules and also the small microcavities that appear in this last phase as a consequence of the extraction of the very small carbides that had precipitated during the tempering heat treatments.

It is worth noting that the fraction of the failure surface associated with the presence of carbides is clearly lower than that observed on the polished surface. This indicates that hot compression failure took place mainly through the dendritic tempered martensite phase. The high stiffness and extreme hardness of the carbides present in these microstructures limit their deformation and promote failure along the weakest phase (tempered martensite), although, as already mentioned, the interphase between carbides and martensite is quite weak and decohesion and carbide extraction also occurs in the course of the failure process.

Fracture toughness

To determine the fracture toughness, the load–displacement curve was registered for each test. These curves are shown in Fig. 8 and the P_Q load value was determined according to the ASTM standard E399. Values of P_Q are used in Eq. (1) to calculate fracture toughness. Table 4 shows a summary of these calculations. Note that increasing the chromium content, the fracture toughness is increased as well. With Cr, we get an increment of in fracture toughness. These specimens verify plane strain conditions.

Table 4 Fracture toughness test results

Heat treatment	HV	K_Q (Mpa $\sqrt{m}$)	P_{max}/P_Q	$B > 2.5\ K_Q/\sigma_y$
T1	725	1,982	2,546	12.5
T2	700	1,800	2,481	13
T3	680	1,777	2,362	9.5
T4	605	1,640	2,069	14

The tests to determine the fracture toughness of high-alloyed steel always gave rise to linear elastic behaviors, characterized by the sudden rupture of the precracked specimens when a critical value of the stress intensity factor was attained. As can be seen in Table 4, all the tests were carried out under plane deformation and restricted plasticity conditions, it thus being possible to determine the fracture toughness of all these products ($K_Q = K_{IC}$).

The fracture toughness of this high speed steel hardly varies with heat treatment, although a slight increase in this property was observed when increasing the hardness of these products via heat treatment. On the other hand, it is interesting to note the high fracture toughness values of these high speed steels compared with the values assigned by the technical literature to conventional martensitic high speed steel, which are in the range 14–20 Mpa $\sqrt{m}$ [8, 9].

Figure 9 shows the general failure pattern of these specimens. As was also revealed in the tensile tests, failure is predominantly intergranular, through the carbide network, (see also Fig. 3). The fractographic detail of Fig. 10 shows the intergranular character of the failure of all these specimens more clearly: an

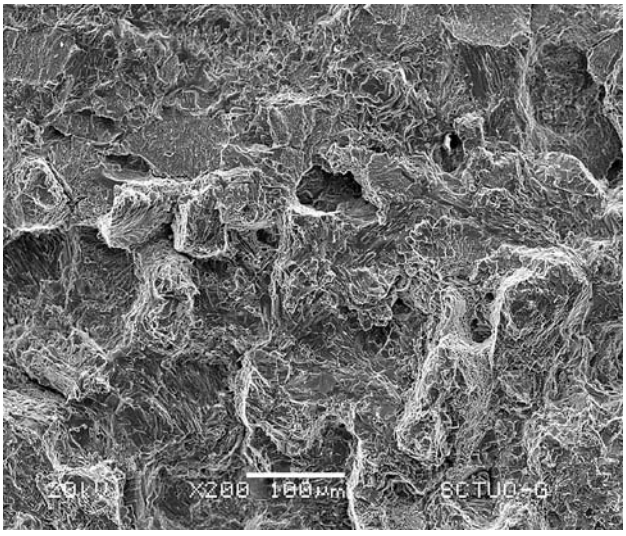

Fig. 9 General fracture pattern of the cast irons in the toughness tests

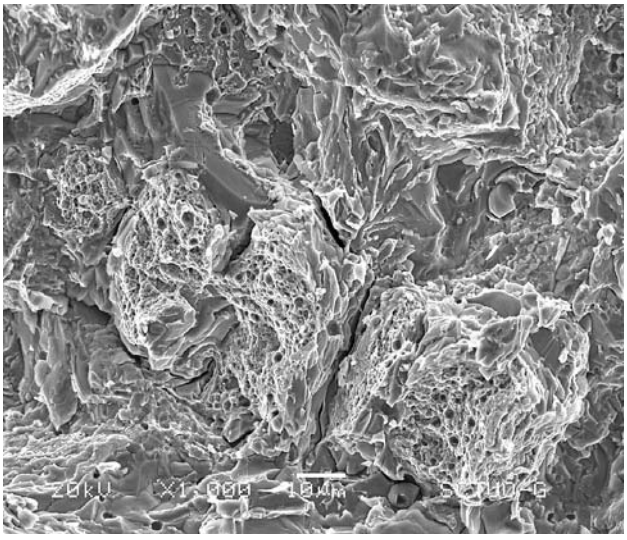

Fig. 10 Fracture toughness test surface detail

almost continuous carbide network that ruptured in a brittle way (cleavage fracture) is seen, with very visible secondary cracks, where the debonding of the carbide/martensite interphase can also be noted. The dendritic phase (tempered martensite), which normally appears isolated (discontinuous areas) in these fractographs, presents a great number of microcavities, giving it the appearance of a ductile failure.

Intergranular brittle fracture due to cleavage or debonding of the eutectic carbides, which constitute the matrix phase of this steel (see Fig. 1), is the most characteristic feature. Similar to the findings of other authors [9–11], and in contrast to what was observed in the hot compression tests, the fraction of carbides on these broken surfaces is clearly larger than that measured on polished surfaces, indicating preferential crack progression along these brittle phases.

On the other hand, the regions of ductile appearance (microcavities smaller than 1 μm) are generated when the crack, as it progresses, crosses the dendritic tempered martensite areas. These are tougher regions that, although not being able to stop the cracks, at least make their normal propagation difficult.

On the other hand, the presence of microcavities in the regions of ductile appearance is the result of initial decohesion and subsequent extraction of the small spherical carbides that have precipitated in these regions in the course of tempering treatments.

The small decrease in fracture toughness observed in the case of the higher tempering temperatures (T3 and T4 treatments) may be attributed to the presence of larger precipitated carbides (carbides grow during tempering), giving rise to larger microcavities.

Some authors [11] report that the presence of secondary carbides is negative from the high speed steel fracture toughness point of view due to dislocation movement inhibition, although a second reason to explain this experimental fact may be that these carbides facilitate the propagation of the cracks by means of their decohesion with the parent phase.

Conclusions

In this study, the effects of tempering heat treatment (hardness modification) on microstructure and fracture properties of an HSS rolls manufactured by vertical centrifugal casting method was investigated and led to the following conclusions:

- After an appropriate heat treatment, these high speed steels are very hard products whose tensile strength decreases along with their hardness on increasing the tempering time and temperature.
- The 500 °C hot compression behavior of these high speed steels is excellent: their strengths are very high and their ductilities normally exceed 10, a linear relation having been obtained between their compressive strength at 500 °C and their room temperature hardness.
- The fracture toughness of these high speed steels is relatively high, especially when we compare it with that of conventional materials with similar microstructures. Moreover, this property is hardly modified in the course of normal heat treatments.

- Failure of these products in tensile and fracture toughness tests is intergranular, since it preferentially takes place through the carbide network, due to their brittleness, and also as a result of the interphase decohesion between carbides and the dendritic tempered martensitic phase, which occurs under the strong local stresses, that developed ahead of the crack front. In contrast, failure of the dendritic areas is ductile in appearance, characterised by the presence of a great number of microcavities generated by virtue of the decohesion of small carbides precipitated during the tempering heat treatments.

References

1. Walmag G, Skoszynsky RJ, Breyer JP (2001) Improvement of the work roll performance on the 2050 mm Hot Strip Mill at Iscor Vanderbijipark, La Revue De Metallurgie-CIT, Mars 2001, pp 295–304
2. Rong W, Andren H-O, Wissel H, Dunlop GL (1992) Acta Metall Mater 40:1727
3. Kirn SW, Lee UJ, Woo KD, Kirn DK (2003) Mater Sci Technol 19:1727
4. Tabrett CP, Sare IR (2000) J Mater Sci 35:2069
5. Zhang MX, Kelly PM, Gates JD (2001) J Mater Sci 36:3865
6. Dogan ON, Hawk JA, Laird G (1997) Met Mat Trans 28A:1315
7. Bocalini M, Goldenstein H (2001) Intl Mater Rev 46(2):92–115
8. Kanninen MF, Popelar CH (1985) Advanced fracture mechanics, Ch. 1. Clarendon Press, Oxford
9. Stevens PG, Ivens KP, Harper P (1971) Iron Steel Inst 209:1
10. Ryu JH, Kwon O, Lee PJ, Kirn YM (1992) Iron Steel Inst Jpn 32:1221
11. De Barbadillo JJ, Trozzi CJ (1981) Iron Steel Eng 58:63
12. Judo RR (1979) Iron Steel Eng 56:51
13. Hwang KC, Lee S, Lee HC (1998) Mater Sci Eng A254 (1998) 296
14. Hwang LC, Lee S, Lee HC (1998) Mater Sci Eng A254:296
15. Hwang LC, Lee S, Lee HC (1998) Mater Sci Eng A254:282
16. ASTM E8M92 (1990) Standards test methods of tension testing of metallic materials. Annual Book of ASTM Standards, vol. 03.01, pp 130–140
17. ASTM E9, Standards test methods of compression testing of metallic materials at room temperature. Annual Book of ASTM Standards, vol. 03.01, pp 161–168
18. ESIS P2–92 (1992) ESIS procedure for determining the fracture behaviour of materials, European Structural Integrity Society
19. ASTM E399–90 (1995) Standards test methods for plane-strain fracture toughness of metallic materials. Annual Book of ASTM Standards, vol. 03.01, pp 412–442